

# Dimerization of Formic Acid—An Example of a “Noncovalent” Reaction Mechanism

M. Gantenberg, M. Halupka, and W. Sander\*<sup>[a]</sup>

**Abstract:** The pulse deposition technique allows selectively the isolation of monomeric or dimeric formic acid in argon matrices at 7 K. Warming of matrices containing the monomer M from 7 K to 40 K results in the decrease of M and formation of a dimer B. This dimer is also labile, and further warming finally produces a second dimer A. By comparison with density functional

theory (DFT) calculations and gas phase IR spectra taken from the literature, the latter dimer A was identified as the  $C_{2h}$ -symmetrical cyclic dimer. The unstable

**Keywords:** ab initio calculations • dimerizations • formic acid • IR spectroscopy • matrix isolation • molecular dynamics

dimer B was identified as the acyclic  $C_s$ -symmetrical dimer. An activation energy of  $2.3 \text{ kcal mol}^{-1}$  was calculated for the  $B \rightarrow A$  rearrangement at the B3LYP/6-311++G(d,p) level of theory, which is in qualitative agreement with the experimental finding of a slow thermal reaction under the conditions of matrix isolation.

## Introduction

The knowledge of reaction mechanisms is a prerequisite for the control of chemical reactions, the making and breaking of chemical bonds. While a large amount of experimental information on the formation of covalent bonds has been collected over the last century, studies on mechanisms of the formation of weak noncovalent bonds are much rarer. One field that has been intensely worked on is the folding of proteins from a heterogeneous ensemble of conformers to a unique, homogeneous structure.<sup>[1, 2]</sup> While the mechanism of protein folding is still a challenge to experimentalists and theoreticians, we are interested in small systems that allow one to study the basic principles of the formation of multiple hydrogen bonds with direct spectroscopic methods and quantum-chemical calculations.

Formic acid is one of the simplest systems that forms two hydrogen bonds, and due to its fundamental importance as the simplest carboxylic acid its structure in the gas phase<sup>[3]</sup> and in condensed phases<sup>[4–10]</sup> has been subject to numerous investigations. In the gas phase the monomer and the dimer form an equilibrium, in which the dimer is more stable by  $14 \text{ kcal mol}^{-1}$ .<sup>[11]</sup> In contrast to most other carboxylic acids, which retain the dimeric structure in the crystalline state, the crystal structure of formic acid reveals an infinite, “polymeric” structure.<sup>[12, 13]</sup> The structure of the liquid formic acid is fairly complicated and has been subject to some debate.

Besides the cyclic dimer,<sup>[6]</sup> an acyclic “open” dimer,<sup>[5]</sup> polymeric chains,<sup>[4, 5, 7–10]</sup> or a mixture of several of these species have been postulated to be the main constituent of liquid formic acid.

Matrix isolation is ideally suited to investigate the structures of conformers and weakly bound aggregates. The matrix IR spectrum of monomeric formic acid with only a small contamination by aggregates was published by Reva et al.<sup>[14]</sup> The most stable conformer of formic acid is the *s-trans* conformer, which is  $4.0 \text{ kcal mol}^{-1}$  more stable than the *s-cis* conformer.<sup>[15]</sup> Lundell and co-workers reported on the generation of the *s-cis* conformer by multiphoton IR irradiation of the *s-trans* conformer in low-temperature matrices.<sup>[16]</sup> Here we describe a matrix isolation and computational study on the stepwise dimerization of formic acid.

## Results and Discussion

For the matrix isolation of pure monomeric or dimeric formic acid we used the pulse deposition technique recently developed in our laboratory.<sup>[17]</sup> This technique allows one to generate monomers or dimers by simply changing the duration of a gas pulse (0.5–1% formic acid in argon), expanding from a pressure of 1–2 bar into a high-vacuum system. The gas mixture is trapped on top of a cold spectroscopic window (CsI) at 7 K. A very short pulse duration (typically 0.3 ms) results in the formation of the monomeric acid M in a purity of >95%, while a long pulse duration (20 ms) produces the cyclic dimer A in 96% yield (Figure 1). In Tables 1 and 2 the matrix IR spectra for the

[a] Prof. Dr. W. Sander, M. Gantenberg, M. Halupka  
Lehrstuhl für Organische Chemie II der Ruhr-Universität 44780  
Bochum (Germany)  
Fax: (+49) 234 709-4353  
E-mail: sander@xenon.orch.ruhr-uni-bochum.de

Table 1. Experimental (argon matrix, 10 K) and calculated (B3LYP/6-311++G(d,p)) IR data of monomeric formic acid M.

No.	B3LYP/6-311++G(d,p)			Argon, 10 K		Gas phase <sup>[a]</sup>	
	Sym.	$\nu$ [cm <sup>-1</sup> ]	$I$ [kmol <sup>-1</sup> ]	$\nu$ [cm <sup>-1</sup> ]	$I_{rel}$ <sup>[b]</sup>	$\nu$ [cm <sup>-1</sup> ]	Assignment
9	A'	3737.9	62	3549.9	22.5	3567	$\nu_{OH}$
8	A'	3057.8	44	3066.0	11.6	2941	$\nu_{CH}$
7	A'	1816.0	398	1766.9	98.3	1775	$\nu_{C=O}$
6	A'	1403.3	2	—	—	—	$\delta_{CH}$
5	A'	1293.3	9	1215.2	16.8	1218	$\delta_{COH}$
4	A'	1125.7	278	1103.5	100	1104	$\nu_{CO}$
3	A''	1050.1	2	—	—	—	$\gamma_{CH}$
2	A''	678.4	160	635.1	63.5	640	$\gamma_{OH}$
1	A'	630.2	44	—	—	—	$\delta_{OCO}$

[a] Ref. [3]. [b] Rel. intensity based on the strongest IR absorption.

monomer M and the cyclic dimer A are compared to gas-phase and density functional theory (DFT) calculated data. The carbonyl region of the IR spectrum obtained after the 0.3 ms pulse deposition is dominated by the very intense absorption of the monomer at 1767 cm<sup>-1</sup> with a less intense shoulder at 1765 cm<sup>-1</sup> (Figure 1). This splitting of the carbonyl stretching vibration in solid argon has been described previously<sup>[14]</sup> and is presumably caused by matrix site effects. In addition, two weak absorptions at 1745 and 1728 cm<sup>-1</sup> are observed, which do not belong to monomeric formic acid. The band at 1728 cm<sup>-1</sup> is the most intense absorption after the 20 ms pulse deposition and is readily assigned to the carbonyl vibration of the cyclic formic acid dimer A by comparison to literature data.<sup>[14]</sup> The band at 1745 cm<sup>-1</sup> is found as a weak absorption after both the 0.3 and the 20 ms deposition, and the intensity depends much on the exact conditions of the deposition (window temperature, concentration of formic acid in argon etc.).

In a previous publication<sup>[17]</sup> we tentatively assigned the band at 1745 cm<sup>-1</sup> to unspecified higher aggregates of formic acid. Recently, Spinner questioned this and reassigned the absorption to an acyclic formic acid dimer.<sup>[18]</sup> His main argument was that higher aggregates should be more abundant under the conditions of dimer formation than under conditions which mainly result in monomer formation. To clarify this point, we directly monitored the aggregation of

monomeric formic acid M under the conditions of matrix isolation (Figure 2, Table 3). The aggregation of the monomer M was induced by warming the matrix from 7 K to 40 K with a rate of approximately 1 K min<sup>-1</sup>. At 7 K ( $t=0$ ) the diffusion of formic acid is completely inhibited, and even within a time scale of hours no change in the IR spectrum is observed. At 25 K the intensity of the M absorption at 1767 cm<sup>-1</sup> starts to decrease and the absorption at 1745 cm<sup>-1</sup> gains in intensity, while the absorption at 1728 cm<sup>-1</sup> of dimer A remains almost constant. Further increase of the temperature results in the formation of dimer A, decrease of the monomer M, and

**Abstract in German:** Die gepulste Deposition ermöglicht die selektive Isolation der monomeren oder dimeren Ameisensäure in festem Argon bei 7 K. Erwärmung der mit monomerer Ameisensäure M dotierten Matrizes von 7 auf 40 K führt zur Abnahme von M und Bildung des Dimers B. Dieses Dimer ist labil und weiteres Tempern der Matrix führt schließlich zu einem zweiten Dimer A. Durch Vergleich mit DFT-Rechnungen und Gasphasenspektren aus der Literatur konnte das Dimer A als das cyclische Dimer mit C<sub>2h</sub>-Symmetrie identifiziert werden. Das thermolabile Dimer wurde als ein acyclisches Dimer mit C<sub>s</sub>-Symmetrie identifiziert. Die Aktivierungsbarriere für die B → A Isomerisierung wurde durch Rechnungen auf dem B3LYP/6-311++G(d,p)-Niveau zu 2.3 kcal/mol bestimmt, was in qualitativer Übereinstimmung mit einer langsamen thermischen Isomerisierung unter den Bedingungen der Matrixisolation steht.

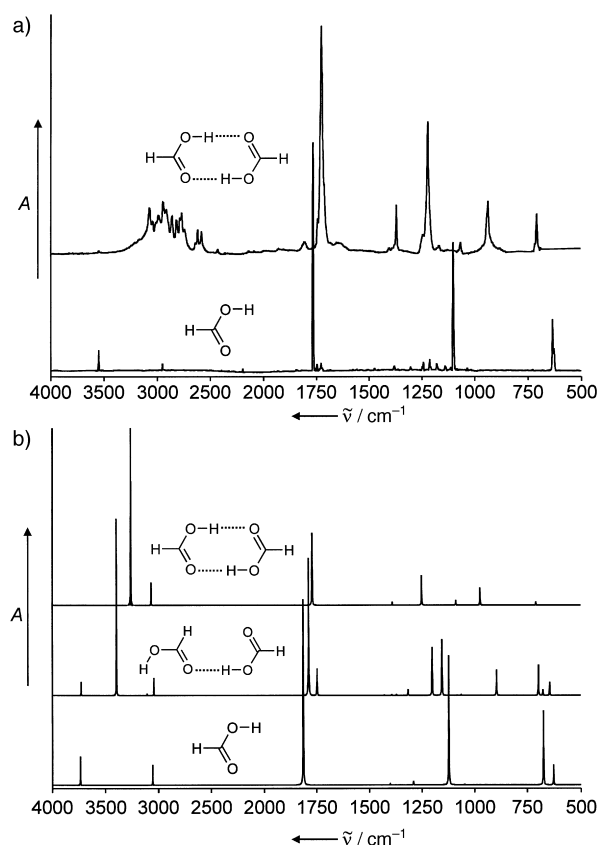


Figure 1. a) IR spectrum of monomeric formic acid (bottom) and formic acid dimer A (top) in argon at 10 K. The matrices were obtained by pulse deposition of 0.5% HCOOH in argon and 0.3 ms pulse duration and 1% HCOOH in argon and 20 ms pulse duration, respectively. b) Spectra of

Table 2. Experimental (argon matrix, 10 K) and calculated (B3LYP/6–311++G(d,p)) IR data of the  $C_{2h}$ -symmetrical dimer A of formic acid.

No.	B3LYP/6–311++G(d,p)		Argon, 10 K		Gas phase <sup>[a]</sup>		
	Sym.	$\nu$ [ $\text{cm}^{-1}$ ]	$I$ [ $\text{km mol}^{-1}$ ]	$\nu$ [ $\text{cm}^{-1}$ ]	$I_{\text{rel}}^{\text{[b]}}$	$\nu$ [ $\text{cm}^{-1}$ ]	Assignment
24	B <sub>u</sub>	3261.5	2154				
23	A <sub>g</sub>	3165.1	0	3100			
22	A <sub>g</sub>	3073.9	0	2430 <sup>[c]</sup>			$\nu_{\text{OH}}/\nu_{\text{CH}}$
21	B <sub>u</sub>	3069.0	276				
20	B <sub>u</sub>	1773.4	879	1728.3	100	1740	$\nu_{\text{C=O}}$
19	A <sub>g</sub>	1706.7	0				
18	A <sub>g</sub>	1461.5	0				
17	B <sub>u</sub>	1438.9	1	1445.6	0.1		$\delta_{\text{OH}}$
16	A <sub>g</sub>	1394.3	0				
15	B <sub>u</sub>	1391.7	44	1371.9	21.8	1364	$\delta_{\text{CH}}$
14	B <sub>u</sub>	1251.6	375	1223.5	56.9	1215	$\nu_{\text{CO}}$
13	A <sub>g</sub>	1248.7	0				
12	A <sub>u</sub>	1091.4	63	1069.3	6.1		$\gamma_{\text{CH}}$
11	B <sub>g</sub>	1070.5	0				
10	A <sub>u</sub>	974.7	207	939.9	22.0	908	$\gamma_{\text{OH}}$
9	B <sub>g</sub>	945.6	0				
8	B <sub>u</sub>	712.0	43	710.6	17.4	699	$\delta_{\text{OCO}}$
7	A <sub>g</sub>	685.1	0				
6	B <sub>u</sub>	260.9	65				
5	B <sub>g</sub>	251.0	0				
4	A <sub>g</sub>	200.2	0				
3	A <sub>u</sub>	176.7	8				
2	A <sub>g</sub>	168.2	0				
1	A <sub>u</sub>	78.0	3				

[a] Ref. [3]. [b] Relative intensity based on the strongest IR absorption. [c] Complex pattern due to Fermi resonance, ref. [3].

monomeric formic acid (bottom), dimer A (middle), and dimer B (top), calculated at the B3LYP/6–311++G(d,p) level of theory.

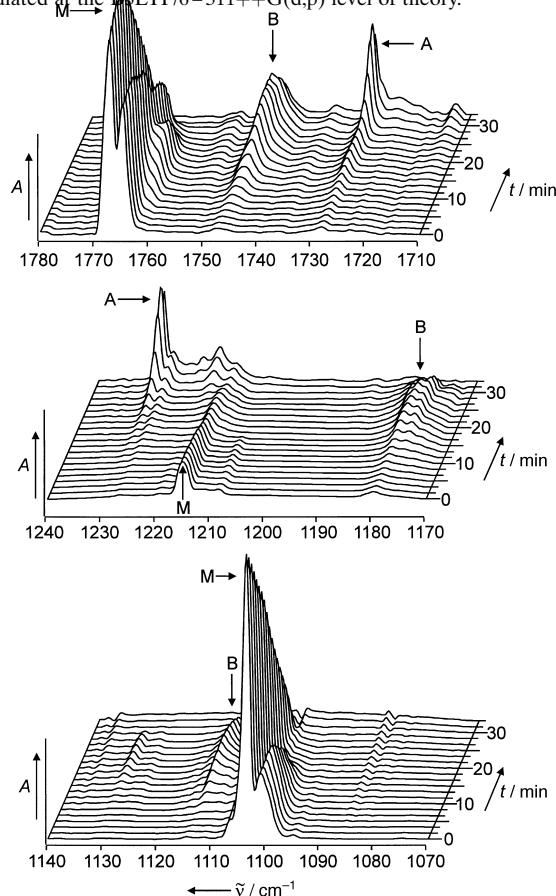


Figure 2. IR spectra of an argon matrix containing formic acid during the slow warm up from 7 K ( $t = 0$  min) to 40 K ( $t = 27$  min). Bands assigned to monomeric formic acid M, dimer A, and dimer B.

above 40 K the band at  $1745 \text{ cm}^{-1}$  also decreases. This observation is in line with the assignment of this absorption at  $1745 \text{ cm}^{-1}$  to an acyclic dimer B which is formed preferentially as the primary product of the formic acid dimerization. The more stable dimer A is produced in a subsequent step from dimer B. The same change of the relative intensities of IR bands as a function of temperature was also observed in the C–OH stretching region. The band at  $1103 \text{ cm}^{-1}$  of the monomer decreases in intensity, the bands at  $1131$  and  $1180 \text{ cm}^{-1}$  of dimer B increase and later decrease, and the band at  $1224 \text{ cm}^{-1}$  of dimer A increases at higher temperatures.

The assignment of the three IR absorptions at  $1745$ ,  $1180$ , and  $1131 \text{ cm}^{-1}$  to the acyclic,  $C_s$ -symmetrical dimer B was confirmed by DFT calculations at the B3LYP/6-311G++G(d,p) level of theory (Table 4). To directly compare the calculated with the experimental IR data, a frequency scaling of 0.973—which exactly adjusts the calculated C=O stretching vibration of the monomer to the experimental value—was applied to all vibrations. With this scaling the C=O stretching vibrations of the  $C_{2h}$ -symmetrical dimer A is predicted at  $1726 \text{ cm}^{-1}$ , close to the experimental value of  $1728 \text{ cm}^{-1}$ . For the C=O stretching vibrations of dimer B two absorptions at  $1742$  (s) and  $1703 \text{ cm}^{-1}$  (m) are predicted. Thus, the strongest band of B should be located between the monomer and dimer A bands, which is in line with the assignment of the band at  $1745 \text{ cm}^{-1}$  in the experimental spectrum to the  $C_s$ -symmetrical dimer B.

Table 3. Experimental (argon matrix, 10 K) and calculated (B3LYP/6–311++G(d,p)) carbonyl stretching frequencies [ $\text{cm}^{-1}$ ]. The calculated absolute intensities [ $\text{km mol}^{-1}$ ] are given in parentheses.

	Monomer M	Dimer A, $C_{2h}$	Dimer B, $C_s$
C=O stretching			
argon, 10 K	1766.9	1728.3	1744.8, –
B3LYP/6–311++G(d,p)	1816.0 (398)	1773.4 (879)	1790.2 (701), 1750.3 (139)
scaled by 0.973 <sup>[a]</sup>	1767.0	1725.5	1741.9, 1703.0
C–OH stretching			
argon, 10 K	1103.5	1223.5	1179.7, 1131.1
B3LYP/6–311++G(d,p)	1125.7 (278)	1251.6 (375)	1203.7 (247), 1157.6 (287)
scaled by 0.973 <sup>[a]</sup>	1095.3	1217.8	1171.2, 1126.4

[a] Scaling factor chosen to reproduce the C=O str. vibration of monomeric formic acid.

Another characteristic absorption of the monomeric formic acid is the very strong C–OH vibration at  $1104 \text{ cm}^{-1}$  (calculation:  $1095 \text{ cm}^{-1}$ ). In the cyclic dimer A this band is shifted to  $1224 \text{ cm}^{-1}$  (calculation:  $1218 \text{ cm}^{-1}$ ). Weak bands at  $1131$  and  $1180 \text{ cm}^{-1}$  are assigned to the acyclic dimer B, again in good agreement with the calculated values ( $1126$  and  $1171 \text{ cm}^{-1}$ , respectively). In Table 4 the complete set of calculated absorptions for dimer B is given.

At the B3LYP<sup>[19, 20]</sup> level of theory using a large triple  $\xi$  basis set (6-311++G(d,p))<sup>[21]</sup> and including zero-point energies

Table 4. Experimental (argon matrix, 10 K) and calculated (B3LYP/6-311++G(d,p)) IR data of the  $C_s$ -symmetrical dimer B of formic acid.

No.	B3LYP/6-311++G(d,p)			Argon, 10 K	Assignment
	Sym.	$\nu$ [ $\text{cm}^{-1}$ ]	$I$ [ $\text{km mol}^{-1}$ ]		
24	A'	3729.9	71		$\nu_{\text{OH}}$
23	A'	3397.2	900		$\nu_{\text{OH}}$
22	A'	3108.0	10		$\nu_{\text{CH}}$
21	A'	3044.2	91		$\nu_{\text{CH}}$
20	A'	1790.2	701	1744.8	$\nu_{\text{C=O}}$
19	A'	1750.3	139		$\nu_{\text{C=O}}$
18	A'	1432.0	2		$\delta_{\text{OH}}$
17	A'	1395.8	7		$\delta_{\text{CH}}$
16	A'	1372.0	8		$\delta_{\text{OH}}$
15	A'	1317.4	33		$\delta_{\text{CH}}$
14	A'	1203.7	247	1179.7	$\nu_{\text{CO}}$
13	A'	1157.6	287	1131.1	$\nu_{\text{CO}}$
12	A''	1087.0	3		$\gamma_{\text{CH}}$
11	A''	1065.5	8		$\gamma_{\text{CH}}$
10	A''	898.6	131		$\gamma_{\text{OH}}$
9	A''	700.2	157		$\gamma_{\text{OH}}$
8	A'	680.0	31		$\delta_{\text{OCO}}$
7	A'	648.5	71		$\delta_{\text{OCO}}$
6	A''	195.7	4		
5	A'	182.6	22		
4	A'	149.5	0		
3	A''	107.5	0		
2	A'	101.4	4		
1	A''	62.8	4		

(ZPE), the stabilization energy of dimer A is calculated to  $-13.3 \text{ kcal mol}^{-1}$ , in good agreement with the experimental value of  $14 \text{ kcal mol}^{-1}$ .<sup>[11]</sup> Since dimer B is stabilized by one

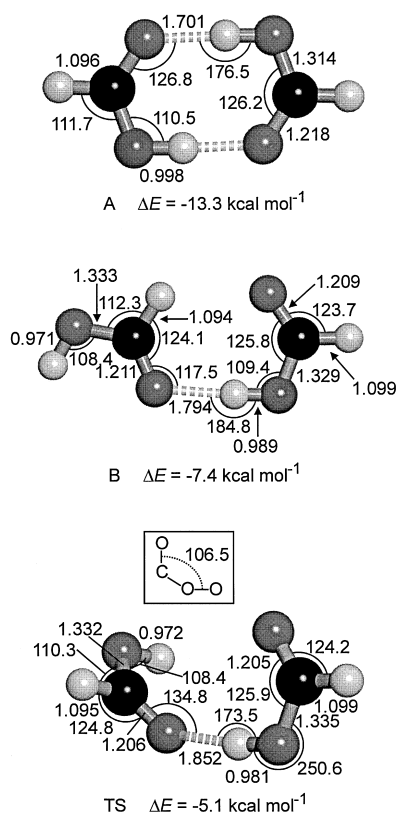


Figure 3. Geometric data of dimer A, dimer B, and the transition state connecting the dimers calculated at the B3LYP/6-311++G(d,p)+ZPE level of theory. Relative energies compared to two molecules of monomeric formic acid.

hydrogen bond only, the stabilization energy of this species is expected to be about half of that of A, again in accordance with the calculated value of  $-7.4 \text{ kcal mol}^{-1}$ . The lower stabilization of B compared to A is also reflected in the increase of the O–O distance across the hydrogen bonds from  $2.698 \text{ \AA}$  in A to  $2.781 \text{ \AA}$  in B (Figure 3). In the acyclic dimer B a small stabilization is expected from the electrostatic interaction of one of the aldehydic H atoms and an adjacent carbonyl group.

The B  $\rightarrow$  A interconversion requires the rotation of one of the formic acid molecules around its C=O bond. This rotation interchanges a strongly interacting OH group with a  $\text{OH} \cdots \text{O}$  distance of  $1.701 \text{ \AA}$  by a weakly interacting H atom with a  $\text{CH} \cdots \text{O}$  distance of  $2.399 \text{ \AA}$ . A DFT calculation (B3LYP/6-31G(d,p)) of the relative energy as a function of this rotation dihedral angle (Figure 4) reveals that a significant barrier of  $3.9 \text{ kcal mol}^{-1}$  separates dimer B from A. With a larger basis set (B3LYP/6-311++G(d,p)) and including ZPE the activation barrier drops to  $2.3 \text{ kcal mol}^{-1}$  (Figure 3) and the transition state is located at a rotation dihedral angle of  $106.5^\circ$ . A barrier of approximately  $2 \text{ kcal mol}^{-1}$  is in qualitative agreement with the observation of a thermal reaction at temperatures as low as  $40 \text{ K}$ . In contrast to B, dimer A is completely stable under the conditions of matrix isolation and even prolonged annealing at  $40 \text{ K}$  did not result in further aggregation.

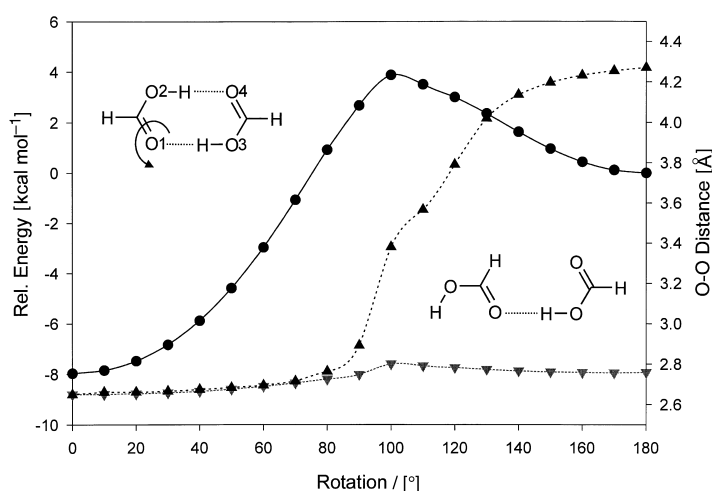


Figure 4. Relative energy and O–O distances during the A  $\rightarrow$  B interconversion of dimeric formic acid via rotation around one of the C=O bonds, calculated at the B3LYP/6-31G(d) level of theory. ●: changes in energy; ▲: O1–O3 distance; ▼: O2–O4 distance.

## Conclusion

Two dimers of formic acid can be trapped in solid argon, the well known cyclic dimer A and the acyclic dimer B. The assignment of IR absorptions of dimer B is in accordance with the suggestion of Spinner<sup>[18]</sup> and was confirmed by the direct observation of the B  $\rightarrow$  A interconversion. Dimer B is a real intermediate with a small activation barrier towards the rearrangement. This species is the building block of solid formic acid and has been postulated to be of importance to liquid formic acid. The matrix experiments clearly demon-

strate that the dimerization of formic acid is a two-step process with dimer B as an intermediate. It is thus reasonable to postulate that low concentrations of B are also present in liquid formic acid.

### Experimental Section

A description of the matrix-isolation technique used is given elsewhere.<sup>[22]</sup> The gas mixtures were prepared in a stainless steel gas-mixing unit. The pulsed deposition unit, built similar to Chen's<sup>[23]</sup> and Maier's<sup>[24]</sup> construction, was described previously.<sup>[17]</sup> To avoid uncontrolled aggregation of the sample in the matrix during the deposition the spectroscopic window has to be held at the lowest temperature possible (7 K). After the deposition, the aggregation is initiated by simply switching off the helium compressor. This leads to a 'free warm up' of the matrix at a rate of approximately 1 K min<sup>-1</sup>. All spectra were recorded by using a Bruker Equinox 55 or IFS 66 FTIR spectrometer with a standard resolution of 0.5 cm<sup>-1</sup>. Calculations were performed on a workstation (Silicon Graphics Origin 2000, operating system Irix 6.4) with the Gaussian 98 program package.<sup>[25]</sup>

### Acknowledgement

This work was financially supported by the Deutsche Forschungsgemeinschaft (SFB 452) and the Fonds der Chemischen Industrie.

- [1] H. S. M. Lu, M. Volk, Y. Kholodenko, E. Gooding, R. M. Hochstrasser, W. F. DeGrado, *J. Am. Chem. Soc.* **1997**, *119*, 7173–7180.
- [2] E. G. Hutchinson, J. M. Thornton, *Protein Sci.* **1994**, *3*, 2207–2216.
- [3] Y. Marechal, *J. Chem. Phys.* **1987**, *87*, 6344–6353.
- [4] R. J. Jakobsen, Y. Mikawa, J. W. Brasch, *Spectrochim. Acta, Part A* **1967**, *23*, 2199–2209.
- [5] P. Waldstein, L. A. Blatz, *J. Phys. Chem.* **1967**, *71*, 2271–2276.
- [6] E. Spinner, *Aust. J. Chem.* **1985**, *38*, 47–68.
- [7] R. C. Paul, R. Sharma, T. Puri, R. Kapoor, *Aust. J. Chem.* **1977**, *30*, 535–541.
- [8] D. Chapman, *J. Chem. Soc.* **1956**, 225–229.
- [9] H. Geisenfelder, H. Zimmermann, *Ber. Bunsenges. Phys. Chem.* **1963**, *67*, 480–486.
- [10] E. Constant, A. Lebrun, *J. Chim. Phys.* **1964**, *61*, 163–173.
- [11] M. D. Taylor, J. Bruton, *J. Am. Chem. Soc.* **1952**, *74*, 4151–4152.
- [12] I. Nahrungbauer, *Acta Crystallogr. Sect. B* **1978**, *34*, 315–318.
- [13] Z. Berkovitch-Yellin, L. Leiserowitz, *J. Am. Chem. Soc.* **1982**, *104*, 4052–4064.
- [14] I. D. Reva, A. M. Plokhhotnichenko, E. D. Radchenko, G. G. Sheina, Y. P. Blagoi, *Spectrochim. Acta, Part A* **1994**, *50A*, 1107–1111.
- [15] W. H. Hocking, *Z. Naturforsch. A* **1976**, *31*, 1113–1121.
- [16] M. Pettersson, J. Lundell, L. Khriachtchev, M. Raesaenen, *J. Am. Chem. Soc.* **1997**, *119*, 11715–11716.
- [17] M. Halupka, W. Sander, *Spectrochim. Acta Part A* **1998**, *54A*, 495–500.
- [18] E. Spinner, *Spectrochim. Acta Part A* **1999**, *55*, 1819–1825.
- [19] A. Becke, *J. Chem. Phys.* **1993**, *98*, 5648–5652.
- [20] C. Lee, W. Yang, R. G. Parr, *Phys. Rev. B: Condens. Matter* **1988**, *37*, 785–789.
- [21] R. Krishnan, J. S. Binkley, R. Seeger, J. A. Pople, *J. Chem. Phys.* **1980**, *72*, 650–654.
- [22] W. W. Sander, *J. Org. Chem.* **1989**, *54*, 333–339.
- [23] D. W. Kohn, H. Clauberg, P. Chen, *Rev. Sci. Instrum.* **1992**, *63*, 4003–4005.
- [24] G. Maier, T. Preiss, H. P. Reisenauer, *Chem. Ber.* **1994**, *127*, 779–782.
- [25] M. J. Frisch, G. W. Trucks, H. B. Schlegel, G. E. Scuseria, M. A. Robb, J. R. Cheeseman, V. G. Zakrzewski, J. A. Jr. Montgomery, R. E. Stratmann, J. C. Burant, S. Dapprich, J. M. Millam, A. D. Daniels, K. N. Kudin, M. C. Strain, O. Farkas, J. Tomasi, V. Barone, M. Cossi, R. Cammi, B. Mennucci, C. Pomelli, C. Adamo, S. Clifford, J. Ochterski, G. A. Petersson, P. Y. Ayala, Q. Cui, K. Morokuma, D. K. Malick, A. D. Rabuck, K. Raghavachari, J. B. Foresman, J. Cioslowski, J. V. Ortiz, B. B. Stefanov, G. Liu, A. Liashenko, P. Piskorz, I. Komaromi, R. Gomperts, R. L. Martin, D. J. Fox, T. Keith, M. A. Al-Laham, C. Y. Peng, A. Nanayakkara, C. Gonzalez, M. Challacombe, P. M. W. Gill, B. Johnson, W. Chen, M. W. Wong, J. L. Andres, C. Gonzalez, M. Head-Gordon, E. S. Replogle, J. A. Pople, Gaussian 98, Revision A.3, Pittsburgh PA, **1998**.

Received: October 7, 1999 [F2070]